


Experimental studies of the $\Lambda(1405)$

physics654 – Seminar on exotic multi-quark states

JAKOB KRAUSE

✉ krause@hiskp.uni-bonn.de |  krausejm

Tutor: GEORG SCHELUCHIN

✉ scheluchin@physik.uni-bonn.de

18.06.2021

What is special about the $\Lambda(1405)$?

- ▶ mass does not fit well into constituent quark models
- ▶ invariant mass distribution (line shape) differs significantly from usual BREIT-WIGNER shape
- ▶ candidate for an exotic multiquark state (bound system of $\bar{K}N$) since its mass lies just below production threshold

there are many different theoretical approaches to explain this behavior
→ need for more experimental data!

Table of contents

1. Experimental setup
2. Line-shape measurement
 - Event selection
 - Measurements and analysis
 - Interpretation of results
3. Spin-parity measurement
4. Conclusion

1. Experimental setup

2. Line-shape measurement

Event selection

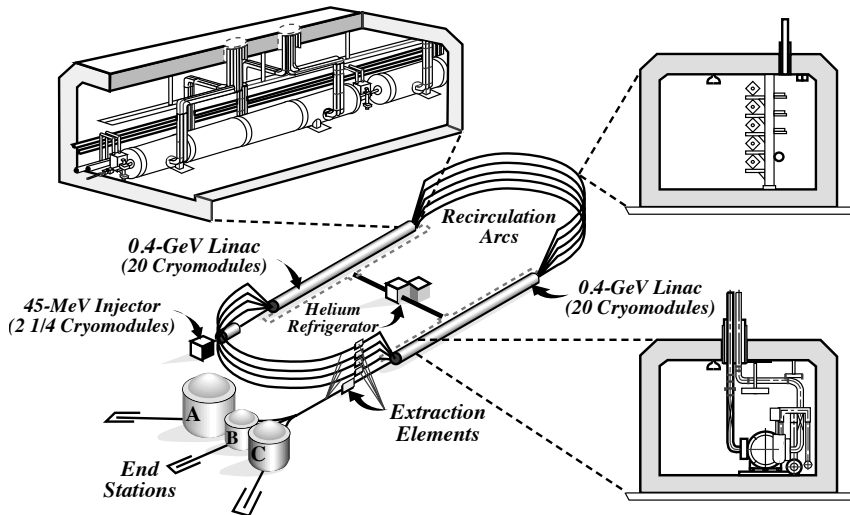
Measurements and analysis

Interpretation of results

3. Spin-parity measurement

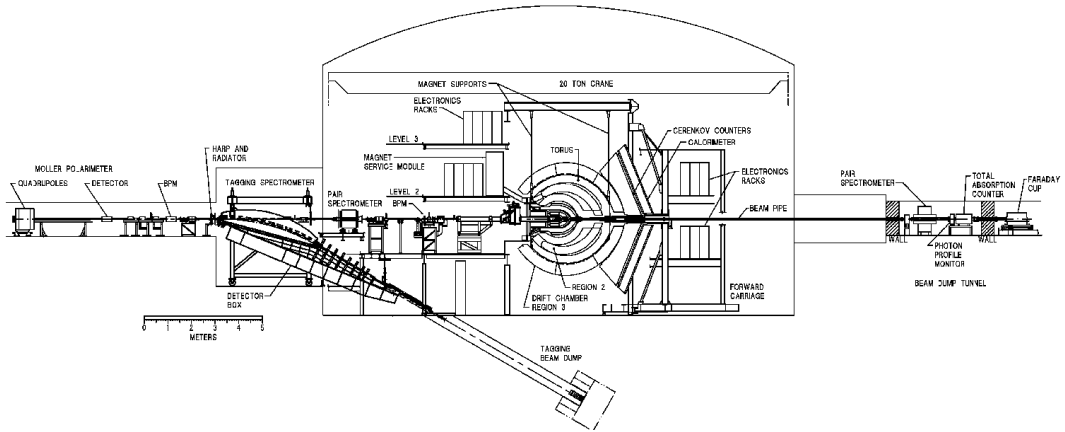
4. Conclusion

Continuous Electron Beam Accelerator Facility (CEBAF)



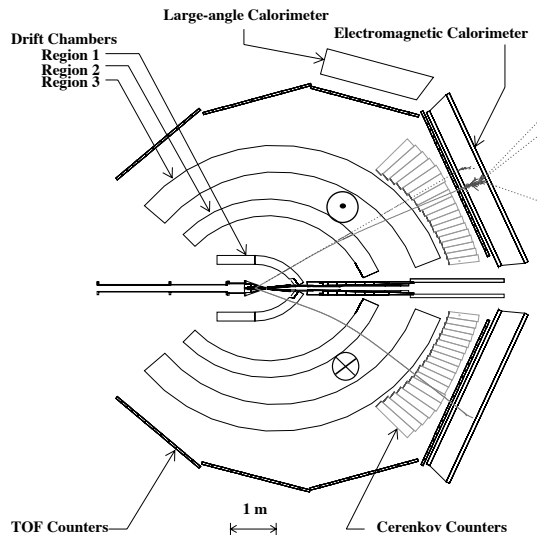
CEBAF layout at Jefferson Lab, [Mecking et al. 2003]

Continuous Electron Beam Accelerator Facility (CEBAF)



Overview of the CLAS detector setup, including the tagger, [Mecking et al. 2003]

CEBAF Large Acceptance Spectrometer (CLAS)



CLAS layout at Jefferson Lab, [Mecking et al. 2003]

1. Experimental setup

2. Line-shape measurement

Event selection

Measurements and analysis

Interpretation of results

3. Spin-parity measurement

4. Conclusion

1. Experimental setup

2. Line-shape measurement

Event selection

Measurements and analysis

Interpretation of results

3. Spin-parity measurement

4. Conclusion

Reaction kinematics

Reaction	Strong Final State	Undetected $K^+ p \pi^-(X)$	Particles X $K^+ \pi^+ \pi^-(X)$
$\gamma + p \rightarrow K^{++}$	$\begin{cases} \Lambda(1405) \\ \Lambda(1520) \end{cases}$		
	$\begin{array}{l} \sim 33\% \rightarrow \Sigma^+ \pi^- \\ \sim 33\% \rightarrow \Sigma^0 \pi^0 \\ \sim 33\% \rightarrow \Sigma^- \pi^+ \end{array}$	$\begin{array}{l} \pi^0 (52\%) \\ \pi^0 \gamma (64\%) \end{array}$	$\begin{array}{l} n (48\%) \\ n (100\%) \end{array}$
$\gamma + p \rightarrow K^+ + \Sigma^0(1385)$	$\begin{array}{l} 6\% \rightarrow \Sigma^+ \pi^- \\ 6\% \rightarrow \Sigma^- \pi^+ \\ 87\% \rightarrow K^+ \Lambda \pi^0 \end{array}$	$\begin{array}{l} \pi^0 (64\%) \\ \pi^0 \gamma (64\%) \end{array}$	
$\gamma + p \rightarrow K^{*+} + \Sigma^0$		$\pi^0 \gamma (64\%)$	
$\gamma + p \rightarrow K^{*0} + \Sigma^+$		$\pi^0 (52\%)$	$n (48\%)$

$$\Sigma^+ \rightarrow p \pi^0$$

$$\Sigma^+ \rightarrow n \pi^+$$

$$\Sigma^0 \rightarrow \gamma \Lambda$$

$$\Sigma^- \rightarrow n \pi^-$$

$$\Lambda \rightarrow p \pi^-$$

$$\rightarrow \gamma p \pi^-$$

Possible and studied reactions in the analysis of the lineshapes of $\Lambda(1405)$, [Moriya, Schumacher, Adhikari et al. 2013]

Event selection

two sets of reactions that the detector sees

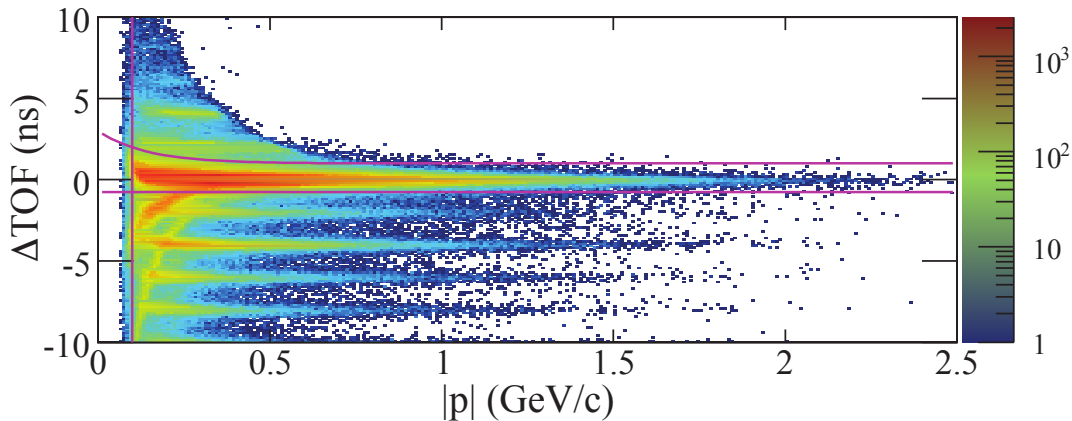
1. $K^+ p \pi^-(X)$
2. $K^+ \pi^+ \pi^-(X)$

there are many cuts that can be made that apply to both

Initial selection of particles

- ▶ particle identification using TOF counters and momentum measurements
- ▶ kinematic cuts from MONTE CARLO

Event selection – Particle identification



ΔTOF for π^+ @ $2.35 < W < 2.45$ GeV, applied cuts are shown in magenta. [Moriya, Schumacher, Adhikari et al. 2013]

Event selection

Binning of data

the data was divided:

- ▶ 10 bins in $W = \sqrt{s}$ dividing 2 GeV to 3 GeV in steps of 100 MeV
- ▶ 20 bins in $\cos \theta_{\text{CMS}}^{K^+}$ dividing -1 to 1 in steps of 0.1

→ the following analysis was performed independently in every bin of energy and angle!

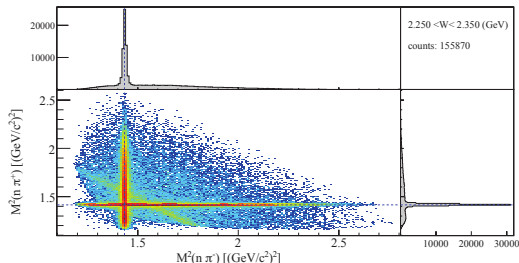
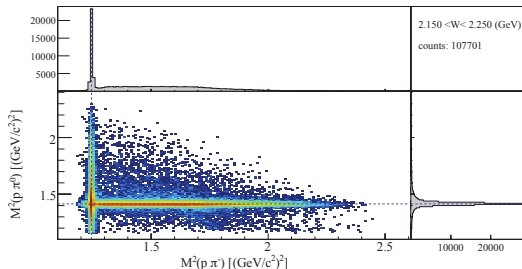
Event selection

extracting $\Lambda\pi^0$ and $\Sigma^+\pi^-$

- reminder: $\Lambda \rightarrow p\pi^-, \Sigma^+ \rightarrow p\pi^0$
- final state particles: $K^+p\pi^-(\pi^0)$
- determine p_π via missing mass fit
- apply cuts based on fits to the invariant masses $M_{p\pi^-}$ and $M_{p\pi^0}$

extracting $\Sigma^+\pi^-$ and $\Sigma^-\pi^+$

- reminder: $\Sigma^\pm \rightarrow n\pi^\pm$
- final state particles: $K^+\pi^+\pi^-(n)$
- determine p_n via missing mass fit
- apply cuts based on fits to the invariant masses $M_{n\pi^\pm}$

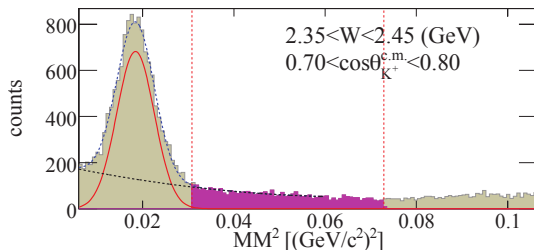


DALITZ-like plots of the above mentioned invariant masses, [Moriya, Schumacher, Adhikari et al. 2013]

Event selection

extracting $\Sigma^0\pi^0$

- reminder: $\Sigma^0 \rightarrow \gamma\Lambda \rightarrow \gamma p\pi^-$
- final state particles: $K^+p\pi^-(\gamma\pi^0)$ - missing mass fit is not applicable here: demand the missing mass is sufficiently greater than m_π
- make cuts based on the invariant mass $M_{p\pi^-}$
- now the missing mass ($\gamma p \rightarrow K^+X$) gives the $\Sigma^0\pi^0$ lineshape



Missing mass of the reaction $\gamma p \rightarrow K^+p\pi^-(X)$, selection range in magenta. [Moriya, Schumacher, Adhikari et al. 2013]

1. Experimental setup

2. Line-shape measurement

Event selection

Measurements and analysis

Interpretation of results

3. Spin-parity measurement

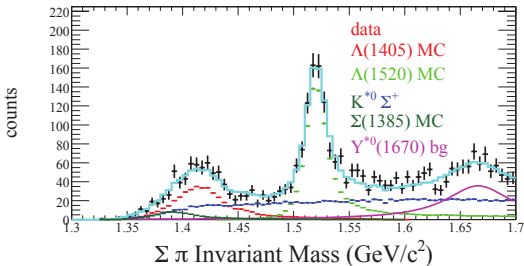
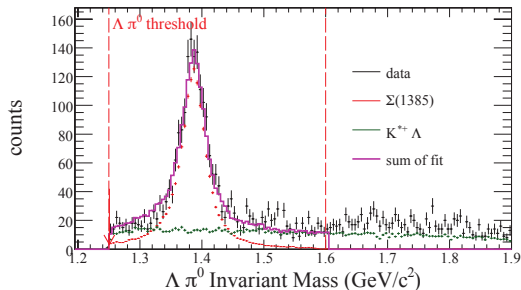
4. Conclusion

Measurements and analysis

- ▶ now the signal regions have been established
- ▶ the true lineshape of the $\Lambda(1405)$ has to be extracted from the vast of reactions \rightarrow any other contributions have to be subtracted
- ▶ strategy: use of MONTE-CARLO fits to the data, simulating the contribution of other resonances using the PDG widths and masses

Measurements and analysis

some fit results:



Sample fit results of invariant mass spectra for a single bin in energy and angle, [Moriya, Schumacher, Adhikari et al. 2013]

1. Experimental setup

2. Line-shape measurement

Event selection

Measurements and analysis

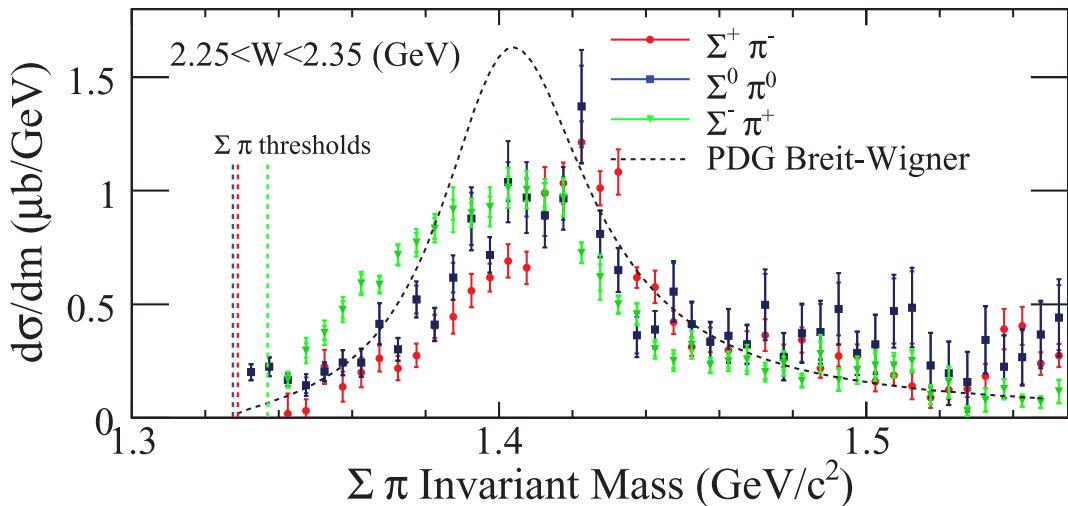
Interpretation of results

3. Spin-parity measurement

4. Conclusion

Interpretation of the results

having subtracted all unwanted reactions, one can obtain the true $\Lambda(1405)$ lineshapes:

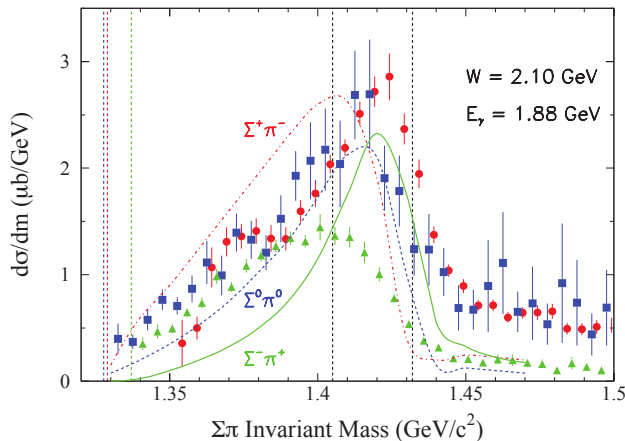


Lineshapes of the $\Lambda(1405)$ for the 3 different decay channels and the PDG BREIT-WIGNER. The data were summed over all angles for better statistics. [Moriya, Schumacher, Adhikari et al. 2013]

Interpretation of the results

there are in fact predictions of the lineshapes differing by decay channel [Nacher et al. 1999].

→ main idea: not one amplitude, but two due to isospin decomposition.



Lineshapes of the $\Lambda(1405)$ for the 3 different decay channels and the prediction of [Nacher et al. 1999], [Moriya, Schumacher, Adhikari et al. 2013]

Interpretation of the results

MORIYA ET AL. saw two main reasons for the lineshapes differing from a simple BREIT-WIGNER:

1. isospin decomposition
2. channel coupling between the detected $\Sigma\pi$ and $N\bar{K}$ final states

Isospin decomposition

let

$$|t_I|^2 = |\langle I, 0 | T^{(I)} | \gamma p \rangle|^2,$$

then we can write (neglecting $I = 2$ using CGK)

$$|T_{\pi^-\Sigma^+}|^2 = \frac{1}{3}|t_0|^2 + \frac{1}{2}|t_1|^2 - \frac{2}{\sqrt{6}}t_0t_1 \cos \phi_{01}$$

$$|T_{\pi^0\Sigma^0}|^2 = \frac{1}{3}|t_0|^2$$

$$|T_{\pi^+\Sigma^-}|^2 = \frac{1}{3}|t_0|^2 + \frac{1}{2}|t_1|^2 + \frac{2}{\sqrt{6}}t_0t_1 \cos \phi_{01}$$

Channel coupling

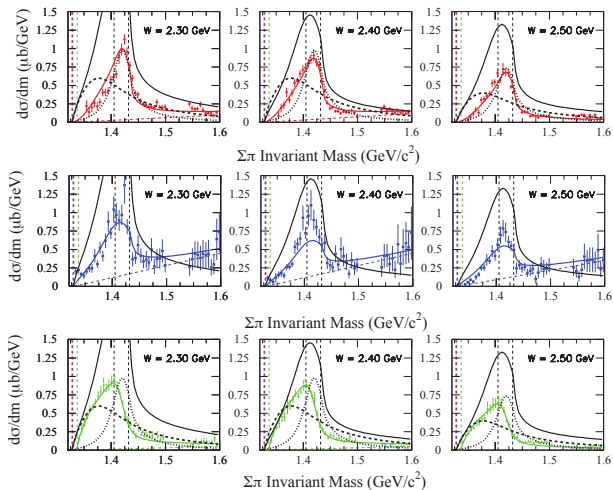
the t_I are described by one or two BREIT-WIGNER amplitudes with mass dependent widths Γ

→ modify the amplitude preserving analyticity [Flatté 1976] including the $N\bar{K}$ decay channel available at threshold

$$m_K + m_p \approx 1434 \text{ MeV}$$

Interpretation of results

fits with two $I = 1$ and one $I = 0$ amplitudes lead to best agreement with measured data



Data and fits for $\Sigma^a\pi^b$, $\{a,b\} \in \{+-, 00 - +\}$ for different bins in W . $I = 0$ (solid black), narrow $I = 1$ (dotted black) and wide $I = 1$ (dashed black). Background dashed. [Moriya, Schumacher, Adhikari et al. 2013]

1. Experimental setup
2. Line-shape measurement
 - Event selection
 - Measurements and analysis
 - Interpretation of results
3. Spin-parity measurement
4. Conclusion

Theoretical basics I

The $\Lambda(1405)$ is so far (mostly) assumed to have $J^P = \frac{1}{2}^-$, but this has not been determined experimentally

Measuring spin

- ▶ consider the strong decay $Y^* \rightarrow Y\pi$, with J^P the spin and parity of Y^*
- ▶ the $Y\pi$ angular distribution will only depend on J

$$I(\theta_Y) = \text{const.} \qquad J = 1/2$$

$$I(\theta_Y) \propto 1 + \frac{3(1-2p)}{2p+1} \cos^2 \theta_Y \qquad J = 3/2,$$

where θ_Y is the polar angle of the decay direction of Y in the Y^* rest frame, p describes the fraction of spin projections along the z axis

- ▶ uniform decay pattern is best evidence for spin $J = 1/2$

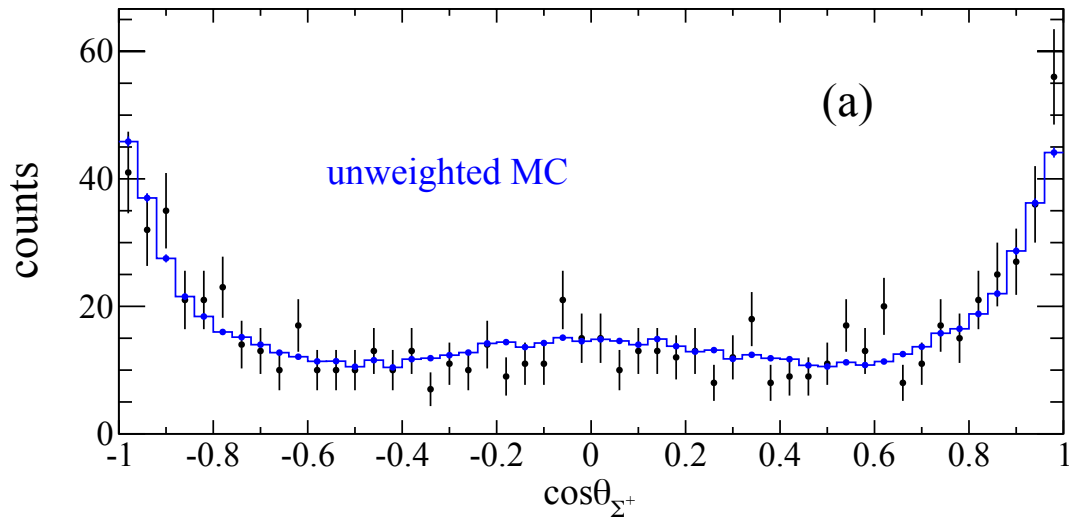
[Moriya, Schumacher, Aghasyan et al. 2014]

Measurements and analysis I

Analysis procedure

- ▶ plot the angular distribution of the projections $\cos \theta_{\Sigma}$ for each bin
- ▶ test each spin hypothesis using MONTE-CARLO maximum likelihood fits, which employ angular decay probability distributions according to each hypothesis for $\Sigma\pi$
- ▶ compare each hypothesis by calculating a χ^2 probability

Measurements and analysis I



Distribution of decay angle of the σ^+ with MONTE-CARLO fit using flat templates [Moriya, Schumacher, Aghasyan et al. 2014]

Theoretical basics II

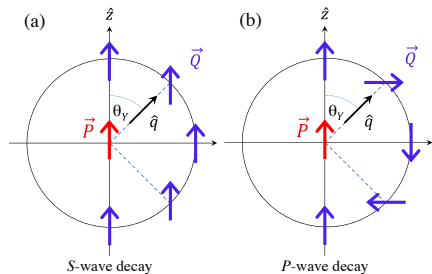
Measuring parity

- ▶ the key to accessing the parity lies in determining the Polarization transfer to the decay product Y which we will denote \mathbf{Q}
- ▶ the angular distribution of \mathbf{Q} will only depend on \mathbf{P}

$$\mathbf{Q}(\theta_Y) = \text{const.} \quad J^P = 1/2^-$$

$$\mathbf{Q}(\theta_Y) = -\mathbf{P} + 2(\mathbf{P} \cdot \mathbf{q})\mathbf{q} \quad J^P = 1/2^+$$

- ▶ \mathbf{Q} can be measured from weak decay angular distribution of Y



Polarization transfer in the strong decay $Y^* \rightarrow Y\pi$, [Moriya, Schumacher, Aghasyan et al. 2014]

[Moriya, Schumacher, Aghasyan et al. 2014 and Ref. therein]

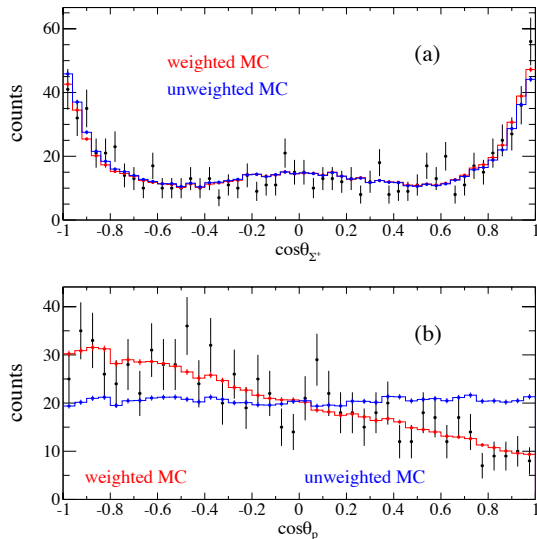
Measurements and analysis II

Analysis procedure

- ▶ plot the angular distribution of the projections $\cos \theta_p$ for each bin
- ▶ determine the polarization using MONTE-CARLO fits
- ▶ determine $Q_z(\cos \theta_{\Sigma^+})$ to get the parity (const. for $P = -$ quadratic for $P = +$)

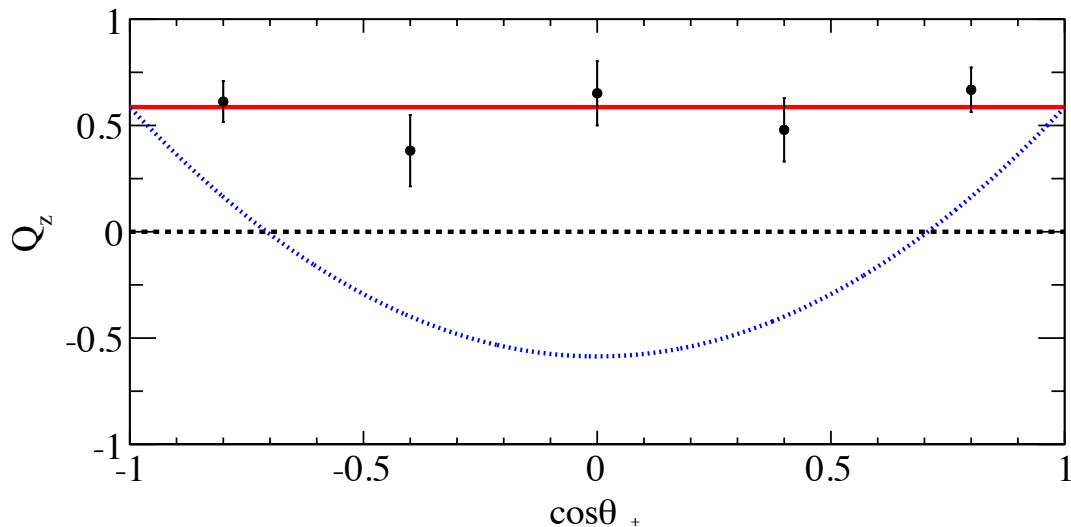
Result: data is consistent with $J^P = 1/2^-$ but does in principle not rule out $J^P = 3/2^+$. $1/2^+$ and $3/2^-$ hypotheses can be discarded.

Measurements and analysis II



Distributions of the projections of (a) $\cos \theta_{\Sigma^*}$ and (b) $\cos \theta_p$ @ $2.65 < W < 2.75$ GeV and $0.70 < \cos \theta < 0.80$, [Moriya, Schumacher, Aghasyan et al. 2014]

Measurements and analysis II



Angular distribution of the polarization Q_z @ $2.65 < W < 2.75$ GeV and $0.70 < \cos\theta < 0.80$. Red: average, blue: expectation for P -wave decay. [Moriya, Schumacher, Aghasyan et al. 2014]

1. Experimental setup
2. Line-shape measurement
 - Event selection
 - Measurements and analysis
 - Interpretation of results
3. Spin-parity measurement
4. Conclusion

Conclusion





Lineshape measurement

- ▶ the CLAS detector was used to study $\gamma p \rightarrow K^+ \Lambda(1405)$
- ▶ after selecting the correct events the true lineshape was extracted using MONTE-CARLO sim. of the yield of other resonances
- ▶ the lineshapes in different decay channels differ from each other and from a simple BREIT-WIGNER
- ▶ a phenomenological isospin decomposition model was able to describe the data

Spin parity measurement

- ▶ the angular distribution of the decay $\Lambda(1405) \rightarrow \Sigma^+ \pi^-$ was studied
- ▶ the angular distributions were tested against various J^P hypotheses
- ▶ the data is consistent with $J^P = 1/2^-$ but does not exclude $J^P = 3/2^+$

References

-  Flatté, S.M. (1976). ‘Coupled-channel analysis of the $\pi\eta$ and $K\bar{K}$ systems near $K\bar{K}$ threshold’. In: *Physics Letters B* 63.2, pp. 224–227. ISSN: 0370-2693. DOI: [https://doi.org/10.1016/0370-2693\(76\)90654-7](https://doi.org/10.1016/0370-2693(76)90654-7). URL: <https://www.sciencedirect.com/science/article/pii/0370269376906547>.
-  Mecking, B.A. et al. (2003). ‘The CEBAF large acceptance spectrometer (CLAS)’. In: *Nuclear Instruments and Methods in Physics Research Section A: Accelerators, Spectrometers, Detectors and Associated Equipment* 503.3, pp. 513–553. ISSN: 0168-9002. DOI: [https://doi.org/10.1016/S0168-9002\(03\)01001-5](https://doi.org/10.1016/S0168-9002(03)01001-5). URL: <https://www.sciencedirect.com/science/article/pii/S0168900203010015>.
-  Moriya, K., R. A. Schumacher, K. P. Adhikari et al. (Mar. 2013). ‘Measurement of the $\Sigma\pi$ photoproduction line shapes near the $\Lambda(1405)$ ’. In: *Phys. Rev. C* 87 (3), p. 035206. DOI: [10.1103/PhysRevC.87.035206](https://doi.org/10.1103/PhysRevC.87.035206). URL: <https://link.aps.org/doi/10.1103/PhysRevC.87.035206>.
-  Moriya, K., R. A. Schumacher, M. Aghasyan et al. (Feb. 2014). ‘Spin and parity measurement of the $\Lambda(1405)$ baryon’. In: *Phys. Rev. Lett.* 112 (8), p. 082004. DOI: [10.1103/PhysRevLett.112.082004](https://doi.org/10.1103/PhysRevLett.112.082004). URL: <https://link.aps.org/doi/10.1103/PhysRevLett.112.082004>.

Back-up: Continuous Electron Beam Accelerator Facility (CEBAF)

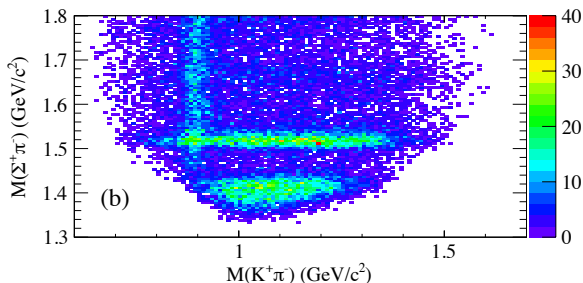
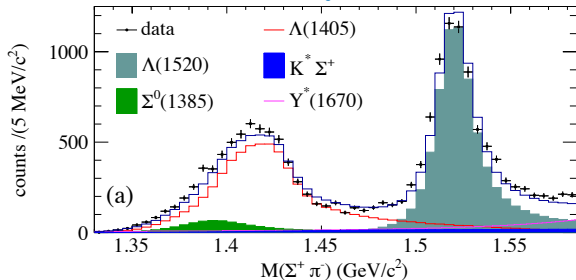
How can we access $\Lambda(1405)$ with this setup?

- ▶ employ radiator target for the electrons
- ▶ generate high energy photons using the *bremsstrahlung* process
- ▶ shoot high energy photons on proton target (LH2)
- ▶ then we can observe $\gamma p \rightarrow K^+ \Lambda(1405)$ while knowing p_γ, p_p

Back-up: Spin-Parity – Measurements and analysis

Event selection

- ▶ select kinematic region where the $\Sigma\pi$ invariant mass is dominated by the $\Lambda(1405) \rightarrow M_{\Sigma\pi} \in 1.30 \text{ GeV to } 1.45 \text{ GeV}$
- ▶ inspect nine bins in energy and angle, namely with CM energy at 2.6, 2.7 and 2.8 GeV and the three forwardmost kaon angle bins each



$\Sigma\pi$ and $K\pi$ invariant mass in the vicinity of the $\Lambda(1405)$, [Moriya, Schumacher, Aghasyan et al. 2014]